Materials Science-Poland, *Vol. 26*, *No. 3*, *2008*

Lifetime prediction in creep-fatigue environment

M. H. SABOUR[1*], R. B. BHAT[2]

[1] Department of Mechanical Engineering, Semnan University, Semnan, Iran

[2] Department of Mechanical and Industrial Engineering,
Concordia University, Montreal, Quebec, Canada

The creep-fatigue interaction has been studied and innovative mathematical models are proposed to predict the operating life of aircraft components, specifically gas turbine blades subject to creep-fatigue at high temperatures. The historical evolution of the creep-fatigue lifetime prediction is given in order to place the present study in the context. A literature review of the life estimation under creep-fatigue environment is presented.

Key words: *creep-fatigue; lifetime;, constitutive model*

1. Introduction

There is a general tendency towards more severe operating conditions, i.e. higher mechanical loadings and temperatures, in order to increase the efficiency of gas and steam turbines, internal combustion engines, heat exchangers, conventional and nuclear electric power generation equipment and other engineering components and devices. This trend has resulted in starting, growth and interaction of complex damaging processes within the materials of these devices. They can lead to the failure of a component and, consequently, of a whole structure, and thus limit their lifetime. Therefore, a safe assessment of lifetime is very important for the prevention of such failures which may have disastrous consequences; too conservative predictions, however, unnecessarily increase the cost of production and maintenance of such systems.

The blades operate in a damaging environment of high temperatures, centrifugal and gas pressure forces and thermal cycling. These conditions combine at every point in the blade to create an interaction between creep and thermo-mechanical fatigue damage. Because of stress redistribution due to the creep process, it is necessary to include a viscoelastic material model in the finite element analysis. Otherwise, over-conservative creep life predictions are estimated if only the initial elastic stresses are considered. In the current investigation, several aspects of lifetime prediction are of

[*]Corresponding author, e-mail: sabour_mh@yahoo.com

interest. They include the damage due to creep-fatigue interactions, modelling using FEM, and experimental validation. Many researchers have dealt with this issue over the years. The simulation studies on the life-limiting modes of failure, as well as estimating the expected lifetime of the blade, using the proposed models have been carried out. Although the scale model approach has been used for quite some time, the thermal scaling (scaled temperature in model and test, with consideration of its restrictions) has been used in this study for the first time.

Many investigators have examined creep-fatigue crack initiation [1–3] and propagation modes [1, 4–11] in general. Some of them focused on studying the effect of specific parameters such as hold time [12, 13] or creep stress effect [14], environment [5, 15], a new evidence of orientation [16, 17], geometry [18], and material parameters [19–21]. Some of them studied metallurgical problems [22] or discussed design rules [23]. In design field, some of them developed a system for assessment [24], used numerical method [25] or damage concept [26] for life prediction, or suggested their own constitutive model [27, 28]. Since it is easier, many of them used thermo-mechanical loading [29–32] for the tests. It was shown in the above studies that the origin of failure under low-cycle fatigue is mainly related to the geometrical discontinuities on the specimen surface and creep-fatigue-environment interactions may enhance the cracking problem. This fact shows the importance of the current study. In low cycle fatigue (LCF) tests, it has been reported that as the hold time is increased, the fatigue life decreases at a fixed test temperature, and the reason for life reduction is reported to be due to the creep effect of stress relaxation which makes an additional plastic strain enlarging the hysteresis loop during hold time. It is reported that creep mechanisms of stress relaxation being the main reasons for fatigue life reduction under creep-fatigue interactions, after a long enough hold time, are the same as that of the monotonic creep [33].

A significant reduction in fatigue life is observed with hold time in compression or in both tension and compression. The influence of tensile hold on fatigue life is more complicated. The mean stress develops during both tensile and compressive hold tests. The scanning electron microscopy (SEM) analysis of fracture surfaces shows that crack initiation and first stage of growth is transgranular but crack growth in a second stage is intergranular [34]. In fact, it has been noted that high-temperature tensile yield strength is an important parameter in studying high-temperature low cycle fatigue properties, crack growth in creep and the effect of cyclic loading on growth in creep-fatigue [10]. To date, there has been no “unified” approach with which the problem of fatigue crack growth at high temperature can be solved in a general manner.

The results show that mixed time and cycle dependent crack growth seems to be the dominant fatigue crack growth mode in the two powder metallurgy (PM) nickel alloys studied, whilst limited creep may be present at the crack tip, particularly under static and long dwell loading conditions [35]. Coffine [36] produced the first significant evidence to suggest that the oxidation is primarily responsible for high temperature low cycle fatigue damage. A variety of studies have been carried out on different alloys, especially directionally solidified superalloy Mar [37, 38], Inconel [39], Co-

base [40, 41], Cr-base [4, 42], Ti-base [43–45], and Al [46]. In the 300 series austenitic stainless steels, such as 304, 316 and 316L used in high temperature applications, many studies have been devoted to understand the creep-fatigue interaction behaviour by employing the hold-time tests [32–55]. It has been observed in these investigations that at relatively high temperatures, continuous cycling endurance is corrupted when a hold-period is included in the cycle. In general, the imposition of holds at tension peak strain tended to be more harmful than those imposed at compression peak strain. Further, there has been conflicting reports on the influence of the tension-hold duration on fatigue life. Hales [56] reported a continuous reduction in life with increase in the length of tension hold-time, while others [13, 57, 58] noted a saturation effect in the life reduction. The creep-fatigue effect in stainless steels is mainly recognized to be due to the inherent weakness of the grain boundaries which lend themselves to the formation of creep induced grain boundary voids that can enlarge into intergranular cavities and cracks [44]. It is acknowledged that the difference between small and long cracks is independent of environment [59]. Several damage rules have been suggested for estimating the cumulative damage under creep-fatigue conditions. The most common approach is based on linear superposition of fatigue and creep damage.

There are divergent opinions regarding which damage approach provides the best basis for life prediction. It is quite clear that a number of variables, such as test temperature, strain range, frequency, time and type of hold, waveform, ductility of the material, and damage characteristics, affect the fatigue life. The conclusions drawn in any investigation may therefore apply only to the envelope of material and test conditions used in that study. The validity of any damage approach has to be examined with reference to the material and service conditions relevant to a specific application.

2. Linear damage summation

The most common approach is based on linear superposition of fatigue and creep damage. Indeed, the mainstay of the present design procedures is the linear life-fraction rule, which forms the basis of the ASME Boiler and Pressure Vessel Code, Section III, Code Case N-47 [63]. This approach combines the damage summations of Robinson for creep [64] and of Miner for fatigue [65] as follows [66]:

$$\sum \frac{N}{N_f} + \sum \frac{t}{t_r} = D \tag{1}$$

where N/N_f is the cyclic portion of the life fraction, in which N is the number of cycles at a given strain range and N_f is the pure fatigue life at that strain range. The time-dependent creep-life fraction is t/t_r where t is the time at a given stress and temperature, and t_r, is the time to rupture at that stress and temperature. D is the cumulative damage index. Failure is presumed to occur when D = l. If Equation (1) were obeyed, a straight line of the type shown in Fig. 1 between the fatigue- and creep-life fractions

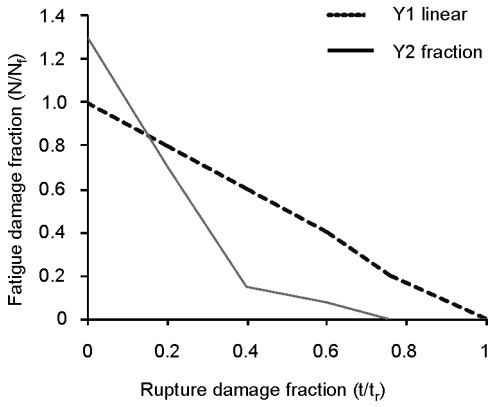

Fig. 1. Creep rupture/low cycle fatigue damage interaction curve for 1Cr–Mo-V rotor steel at 450 °C

would be expected. The life-fraction rule has no mechanistic basis. Its applicability is, therefore, material-dependent. Contrary to experience, it also assumes that tensile and compressive hold periods are equally damaging. The strain softening behaviour, which has been seen in many steels, and the effect of prior plasticity on subsequent creep are not taken into account. Use of virgin material ruptures life to compute creep-life fractions are, therefore, inaccurate. In spite of these limitations, the damage-summation method is very popular because it is easy to use and requires only standard S-N curves and stress-rupture curves.

3. Models of creep-fatigue interaction

As the blades operate at metal temperatures in excess of $0.4T_{\text{melt}}$ in kelvins, creep rupture is clearly a possible failure mode. Also, as the engine cycles through start-up and shut-down with each flight, the transient thermal and body loading stresses cause fatigue damage which can lead to ultimate failure. Thus it is possible to predict the relative amounts of creep and fatigue damage at each point in the blade at each moment of the cycle, which in turn depends upon knowing the stress and temperature conditions at each instant and at spatial point. At start-up, the thermal load was applied to the blade, resulting in a transient thermal stress response. These stresses often reached a maximum value $\sigma_{\max}$ before achieving a steady-state condition. It is therefore necessary to record this maximum stress value at each point over the blade and use it in the fatigue life calculation.

3.1. Model 1

The fluctuating stress can be considered as a varying stress in fatigue-creep model. Since the fluctuating stress is a combination of alternating and mean stresses, it can be

assumed that the part representing the static load can cause creep at elevated temperatures, whereas the alternating part is responsible for fatigue damage. To find the lifetime, the total damage is found by the following model.

3.1.1. Fatigue damage prediction

The Coffine–Manson formula can be applied in elasto-plastic material models. In the case of viscoelasticity, the modified Coffine–Manson formula will be used which includes energy dissipation ΔW as a failure criterion. The number of cycles to failure, N_f, can be calculated from the strain range $\Delta\varepsilon$ using the method of universal slopes. This method has the advantage of using material data obtainable from simple tensile tests. The equation combines the Coffine–Manson law given by

$$\frac{\Delta\varepsilon_p}{2} = \varepsilon_f' \left(2N_f\right)^c \tag{2}$$

where $\Delta\varepsilon_p$ is the plastic strain range, ε_f' is the fatigue ductility coefficient being some fraction (from 0.35 to 1) of the true fracture strain measured in the tension test

$$\varepsilon_f' = \ln\left(\frac{100}{100 - RA}\right)$$

RA is the area reduction [%] at a break, c is the fatigue ductility exponent ranging from about –0.5 to –0.7, N_f is the number of reversals (each cycle equals 2 reversals) and the Basquin law given by

$$\frac{\Delta\varepsilon_e}{2} = \frac{\sigma_f'}{E}\left(2N_f\right)^b \tag{3}$$

where $\Delta\varepsilon_e$ is the elastic strain range, σ_f' is the fatigue strength coefficient approximated by the true fracture stress, equal appromaxitely to s_{ut} + 50 (in units of ksi*), b is the fatigue strength exponent ranging from about –0.06 to –0.14, E is Young's modulus of elasticity. The final formula is given by:

$$\frac{\Delta\varepsilon_{\text{tot}}}{2} = \frac{\sigma_f'}{E}\left(2N_f\right)^b + \varepsilon_f' \left(2N_f\right)^c \tag{4}$$

The total strain range, $\Delta\varepsilon_{\text{tot}}$, can be found by the finite element analysis at each integration point in the model, and the coefficients and the exponents can be found by fatigue tests on the material. For instance, the values for Steel 4340 are

---

*1 ksi = 1.52×10^4 Pa.

$$\varepsilon_f' = 0.58, \quad c = 0.57, \quad b = -0.09, \quad \frac{\sigma_f'}{E} = 0.0062 \tag{5}$$

Using these values, the value of N_f (Eq. (4)), and consequently the fatigue damage parameter, D_f, may be calculated

$$D_f = \frac{n}{N_f} = \frac{t}{t_m N_f} \tag{6}$$

where: n is the number of cycles completed, t is the total analysis time, t_m is the flight duration (mission time),

3.1.2. Creep damage prediction

After the initial transient at start-up, the blade metal temperatures and stresses approach steady-state conditions. However, as these temperatures are typically higher than 40% of T_{melt} [K], creep occurs resulting in stress redistribution. It is therefore important to model the creep process throughout the life of the component. To find the creep damage, it is needed to find the rupture time. For this purpose, the Larson–Miller [67] relation can be used. From the Norton law one can write:

$$\dot{\varepsilon} = \frac{\varepsilon}{t_R} = A_1 \exp\left(-\frac{B_1}{T}\right) \tag{7}$$

From that the rupture time, t_R, is determined as

$$t_R = A_2 \exp\left(\frac{B_2}{T}\right) \tag{8}$$

Taking logarithms on both sides

$$\ln t_R = \ln A_2 + \frac{B_2}{T} = f(\sigma, T) \tag{9}$$

Assuming that $\ln A_2$ is a true constant and that B_2 varies with the stress, the equation can be rearranged to arrive at

$$B_2 = T(\ln t_R - \ln A_2) = T(C_1 + \ln t_R) \tag{10}$$

From the pure creep tests for each material, C can be found. For instance, for steel 4340, it equals to 16.65. The suggested value from the tests is $C_1 = 20$. Consequently, from Eq. (10):

$$\begin{aligned} &P = T(20 + \ln t_R) = f(\sigma, T) \\ &f(\sigma, T) = b_0 + b_1(\ln \sigma) + b_2(\ln \sigma)^2 + b_3(\ln \sigma)^3 \end{aligned} \tag{11}$$

Denoting $Y = \ln t_R$, and $X = \ln\sigma$, we have

$$y = \frac{1}{-17.2T + 460}\left(b_0 + b_1 X + b_2 X^2 + b_3 X^3\right) \tag{12}$$

where: t_R is the rupture time in h, T is temperature in °C, σ is von Mises effective stress inunits of ksi, and b_0, b_1, b_2, b_3 are material constants.

Once t_R is found, the creep damage parameter, D_c, is calculated according to the Robinson rule:

$$D_c = \sum_{i=1}^{N} \left(\frac{\Delta t}{t_R}\right)_i \tag{13}$$

where Δt is the spend time in h, t_R – rupture time in h, i – number of load case.

The total damage parameter is:

$$D_{\text{tot}} = D_c + D_f = \sum_{i=1}^{N}\left(\frac{N}{N_f} + \frac{\Delta t}{t_R}\right)_i \tag{14}$$

The total damage parameter $D_{\text{tot}} \geq 1$ results in failure.

3.2. Model 2

Assuming that the creep behaviour is controlled by the mean stress (σ_m) and that the fatigue behaviour is controlled by the stress amplitude (σ_a), the two processes combine linearly to cause failure. This approach is similar to the development of the Goodman diagram except that instead of an intercept of ultimate stress (σ_u) on the σ_m axis, the intercept used is the creep-limited static stress (σ_{cr}) as shown in Fig. 2.

The creep-limited static stress corresponds either to the design limit on creep strain at the design life or to creep rupture at the design life, depending on which is the governing failure mode. Applying linear failure prediction rule, failure is predicted to occur under combined isothermal creep and fatigue if

$$\frac{\sigma_a}{S_f} + \frac{\sigma_m}{\sigma_{cr}} \geq 1 \tag{15}$$

where: σ_a – alternating stress, σ_m – mean stress, σ_{cr} – creep strength (creep stress for corresponding time to rupture), S_f – fatigue strength.

An elliptic relationship is also shown in Fig. 2. Failure is predicted to occur under combined isothermal creep and fatigue if

$$\left(\frac{\sigma_a}{S_f}\right)^2 + \left(\frac{\sigma_m}{\sigma_{cr}}\right)^2 \geq 1 \tag{16}$$

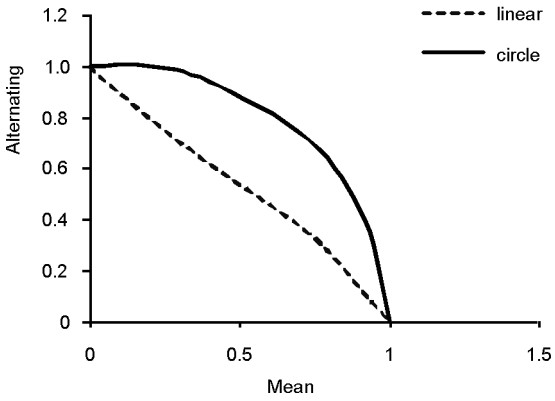

Fig. 2. Failure prediction diagram for combined creep and fatigue at constant temperature

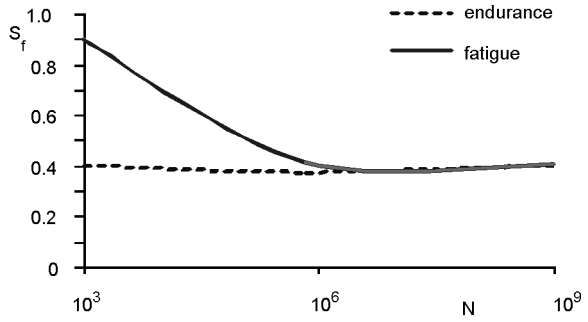

Fig. 3. Failure prediction diagram for creep and fatigue at constant temperature

From Equation (15), σ_a, σ_m and σ_{cr} are known, and S_f can be found. From Fig. 3, we note that:

$$\begin{aligned} &\text{if} \quad S_f > 0.9\sigma_{ut} \quad &&\text{then} \quad N < 10^3 \\ &\text{if} \quad 0.9\sigma_{ut} > S_f > S_e \quad &&\text{then} \quad N = N_{\text{diagram}} \\ &\text{if} \quad S_f < S_e \quad &&\text{then} \quad N > 10^6 \end{aligned} \tag{17}$$

3.3. Model 3

3.3.1. Fatigue damage

It is known that in case of pure fatigue, the damage can be defined as

$$D_f = \sum \frac{N_i}{N_{f_i}} \tag{18}$$

where: N – number of cycles at stress σ_i, N_{f_i} – number of cycles to failure at stress σ_i.

If the process occurs at a constant stress, σ, and constant T

$$D_f = \frac{N}{N_f} \tag{19}$$

where N is the number of cycles at stress a and temperature T, N_f is the number of cycles to failure at stress σ and temperature.

3.3.2. Creep damage

The creep damage under static load can be defined as

$$D_c = \sum \frac{t_i}{t_R} \tag{20}$$

where: t_i is the time spent at stress a and temperature T, t_R – rupture time at stress a, and temperature T and in with hold time for each stress σ, and temperature T_i

$$D_c = \sum \frac{(t_h)_i}{t_{R^i}} \tag{21}$$

where $(t_h)_i$ is the hold time at each temperature T_i. If the process occurs at constant stress, σ, and isothermal condition, T,

$$D_c = \frac{Nt_h}{t_R} \tag{22}$$

where N is the number of cycles with hold time at stress a and temperature T, t_h is the hold time at stress σ and temperature T, t_R is the rupture time at stress σ and temperature T.

3.3.3. Creep-fatigue damage

In creep-fatigue interaction, the total damage is the summation of fatigue damage and creep damage

$$D_t = D_f + D_c = \frac{N}{N_f} + \frac{Nt_h}{t_R} \tag{23}$$

When D_t =1, the failure occurs and hence

$$D_R = \frac{N_R}{N_f} + \frac{N_R t_h}{t_R} = 1 \tag{24}$$

where D_R is the damage at rupture. Consequently,

$$N_R = N_{SF}\left[\frac{1}{\frac{1}{N_f}+\frac{t_h}{t_R}}\right] \tag{25}$$

In Equation (25), N_{SF} is a safety factor which ranges from 0.1 to 1, t_h is known, t_R can be found from Larson-Miller relationship, Equation (12) or from pure creep tests, and N_f can be found from pure fatigue tests or from Eq. (5). Then the number of cycles to failure at creep-fatigue interaction, N_R, can be calculated. Knowing the number of cycles spent in combination of creep and fatigue, the present life status can be found:

$$L_r = 1 - \frac{N}{N_R} \tag{26}$$

where L_r is the remaining life. The remaining number of cycles can be easily calculated as

$$N_r = N_R - N \tag{27}$$

where N_r is the remaining number of cycles.

4. Mechanical testing

One of the most important facts in test is the load waveform. The waveforms shown schematically in Fig. 4 have been applied in the present study. The low-cycle fatigue tests were carried out under closed-loop true temperature control. The tests were performed between 40.04 MPa and 60.10 MPa for fatigue, and creep-fatigue but for the latter 5 s dwell time was applied and the tests were done at 800 °C. For all tests, the specimens with 228.6 mm gauge length and 12.7 mm diameter was used. For the creep test, the average constant stress of 50.07 MPa at 800 °C was applied.

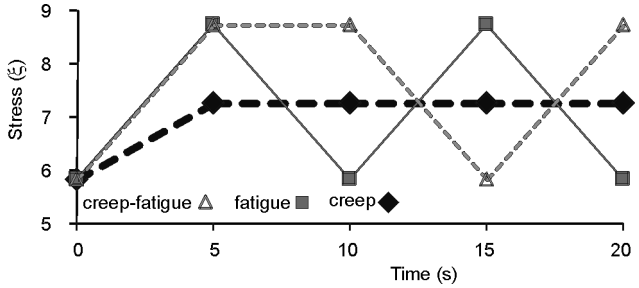

Fig. 4. Load waveform in mechanical testing

The specimen was heated at a temperature gradient along the gauge length not greater than ±2°. Test temperatures varying in the range from 800 °C to 1100 °C were

applied. Ninteen specimens were tested for pure fatigue, pure creep and creep-fatigue interaction, respectively, at various temperatures.

4.1. Test schedule for model 2

Equation (15) has been used to predict failure. Creep-limited static stress, σ_{cr}, in Eq. (15) corresponds either to the design limit on creep strain at the design life or to creep rupture at the design life, depending on which failure mode governs. For this purpose, the tabulated data of material creep test can be used. The following steps are taken:

1. The test temperature, T, is selected.
2. From the creep test data of the material based on design life, and the selected temperature at step 1 as the working temperature, the corresponding creep-limited static stress, σ_{cr} is selected. For instance the a_{cr} at 704.44 °C and for 100 000 h life, is equal to 289.58 MPa.
3. The mean stress, σ_m, and the alternating stress, σ_a, as components of cyclic load are selected.
4. Cyclic load is applied until break and the number of cycles to failure is counted.
5. S_f from Eq. (25) is calculated and the number of cycles to failure is found from Eq. (17).

4.2. Test schedule for model 3

From Equation (25), the following steps are taken:

1. Selecting the temperature, T, between 760 °C and 982.22 °C and the stress, σ, between 206.84 MPa and 275.79 MPa for the test.
2. Selecting the cycle frequency, f, for the fatigue test.
3. Running fatigue test and finding the number of cycles to failure, N_f.
4. Running the static isothermal creep test and finding the rupture time, t_R.
5. Selecting the hold time, t_h, for the cyclic creep test.
6. Running the cyclic creep test at the same frequency of the fatigue one, and finding the number of cycles to failure, N_R.
7. Calculating N_R from Eq. (24).
8. Repeating steps 1–7 for other samples. In the case of using of Eqs. (4) and (24) for fatigue and creep life, respectively, steps 3 and 4 can be ignored.

5. Test analysis

High-temperature strength data are often needed for conditions for which there is no experimental information. This is particularly true of long-time creep and stress-rupture data, where it is quite possible to find that the creep strength to give 1% de-

formation in 100 000 h (11.4 years) is required, although the alloy has been in existence for only 2 years.

Obviously, in such situations extrapolation of the data to long times is required. Reliable extrapolation of creep, creep-fatigue, and stress-rupture curves to longer times can be made only when it is certain that no structural changes occur in the region of extrapolation which would produce a change in the slope of the curve. Since structural changes generally occur in shorter times at higher temperatures, one way of checking on this point is to examine the log-stress-log-rupture life plot at a temperature several hundred degrees above the required temperature. For example, if in 1000 h no change in slope occurs in the curve at about 100 °C above the required temperature, extrapolation of the lower temperature curve as a straight line to 10 000 h is probably safe and extrapolation even to 100 000 h may be possible.

Certain useful techniques have been developed for approximating long-term behaviour based on a series of short-term tests. For instance, the data from creep tests may be cross plotted in a variety of different ways. The basic variables involved are stress, strain, time, temperature, and perhaps strain rate. Any two of these basic variables may be selected as plotting coordinates, with the remaining variables to be treated as parametric constants for a given curve.

One of the commonly used methods for extrapolating short-time creep and creep -fatigue data to long-term applications is the thermal acceleration method. As is a common way in linear viscoelasticity, creep testing guidelines usually dictate that test periods of less than 1% of the expected life are not deemed to give significant results. Tests extending to at least 10% of the expected life are preferred where feasible.

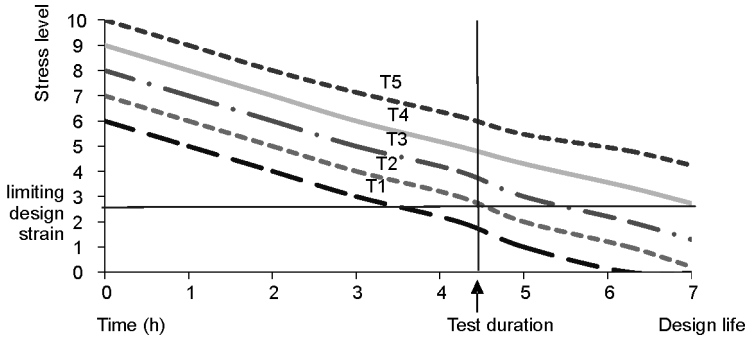

Fig. 5. Thermal acceleration method for creep testing

The thermal acceleration method involves laboratory testing at temperatures much higher than the actual service temperature expected. As shown in Fig. 5, the data are plotted as stress versus time for a family of constant temperatures where the creep strain produced is constant for the whole plot. It may be noted that stress rupture data may also be plotted in this way. As an aid in extrapolation of stress-rupture data several time–temperature parameters have been proposed for trading off temperature for time. The basic idea of these parameters is that they permit the prediction of long-time

rupture behaviour from the results of shorter time tests at higher temperatures at the same stress.

In our tests, we did both upscale and downscale temperature tests. In order to justify the scale model theory specifically in thermal downscaling, the scaled down temperature has been used for the model in comparison with the prototype. On the other hand, in order to run the creep and creep-fatigue test in a time shorter than the reality, tests at the upscale temperature have been carried out. More or less the same upscale force has been applied for the fatigue test to take shorter time than the real case. In the case of applying the real load, it may take ca. 6 months.

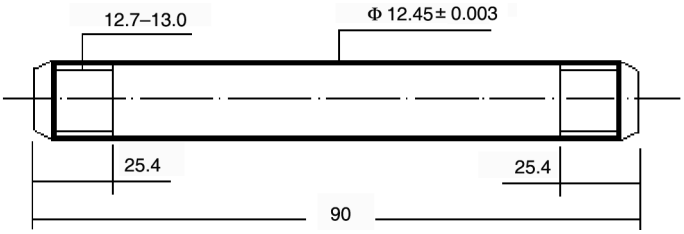

Fig. 6. Geometry of fatigue, creep,
and creep-fatigue specimen, steel 4340 (dimensions in mm)

Material for creep-fatigue tests was Steel 4340. The material and its chemical, physical, and mechanical properties are described in Tables 1–3, respectively. Figure 6 shows the geometry of a specimen used for the creep-fatigue tests.

Table 1. Chemical composition of steel 4340 (in wt. %)

C	Mn	P	S	Si	Cu	Ni	Cr	Mo	Al	V	N	Cd	Sn
0.4	0.75	0.008	0.029	0.26	0.03	1.72	0.87	0.23	0.021	0.001	0.0055	0.002	0.001

Table 2. Physical properties of steel 4340

A [%]	T_{melt} [°C]	ρ [kg/m^3]	α [μm/(m·°C)]	ΔL [%]	ν
36–43	1426.67	7.85×10^3	13.7	13.2	0.29

Table 3. Mechanical properties of steel 4340

S_y [MPa]	E [GPa]	S_{ut} [MPa]	BHN
710	195–205	825–1110	248

The apparatus used in this study was Gleeble-3500 (Fig. 7), a controlled electro-hydraulic thermal-fatigue testing machine with high-precision conduction heating and air-cooling functions [68].

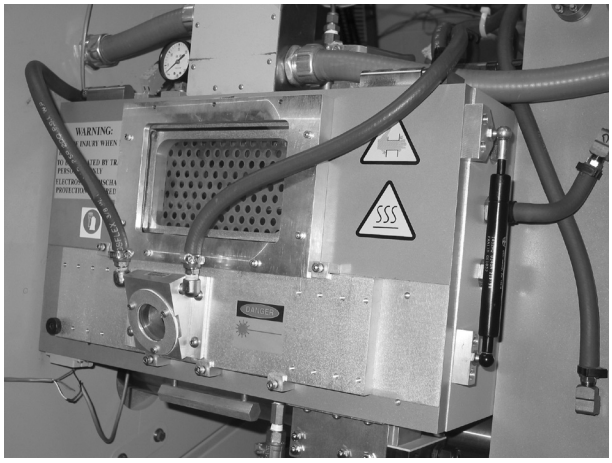

Fig. 7. Gleeble-3500 for various creep, fatigue and creep-fatigue tests
(with the courtesy of National Research Council (NRC) at Boucherville, Quebec)

For axial displacement measurement, Fastar-SP100 sensor from Data Instruments was used which is based on inductance variation. Temperature was measured with a 0.2 mm in diameter thermo-couples welded at the middle and both ends of the specimen. The temperature difference within the gauge length was not greater than ±2 °C to the set temperature throughout the duration of a test. In the creep-fatigue tests, force was computer-controlled by the same triangular waveform cycling. The same temperature was used for creep, and creep-fatigue tests, using the output of the thermocouple.

The waveforms shown in Fig. 4 were applied in the tests, and were done using the testing facilities at the National Research Council (NRC), Boucherville, Quebec S_f= 807.18 MPa, which is greater than $0.9S_{ut}$ = 742.5 MPa. It can be concluded that $N_f < 10^3$.

5.1. Test results

5.1.1. Model 1

For creep, four tests were carried out on a sample of steel 4340 90 mm long, 12.7 mm in diameter which was cleaned and annealed at 248 BHN. For creep test the waveform shown in Fig. 8 has been applied. Indeed we could just apply the temperature and the force of 6.31 KN which is equivalent to stress of 50.09 MPa (Fig. 9). The creep strains at various temperatures at a constant load (6.31 KN) are shown in Figs. 10–13.

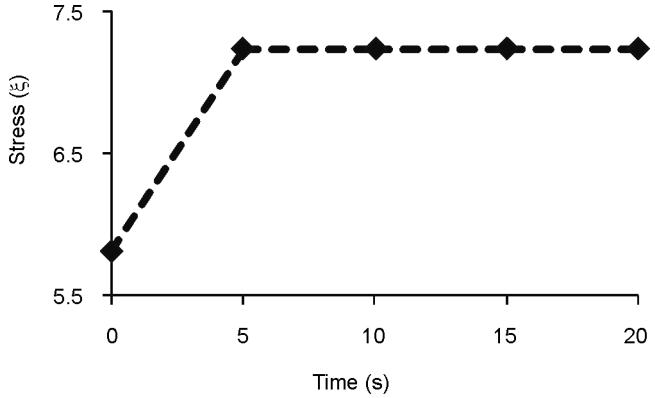

Fig. 8. Stress waveform for creep tests

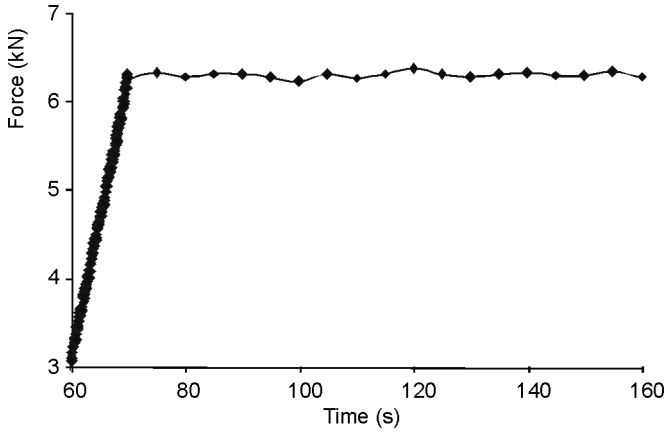

Fig. 9. Force waveform for creep tests

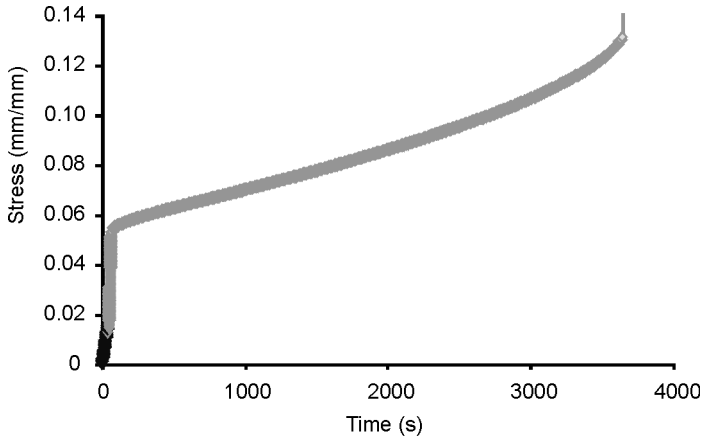

Fig. 10. Creep strain vs. time at 800 °C in creep test

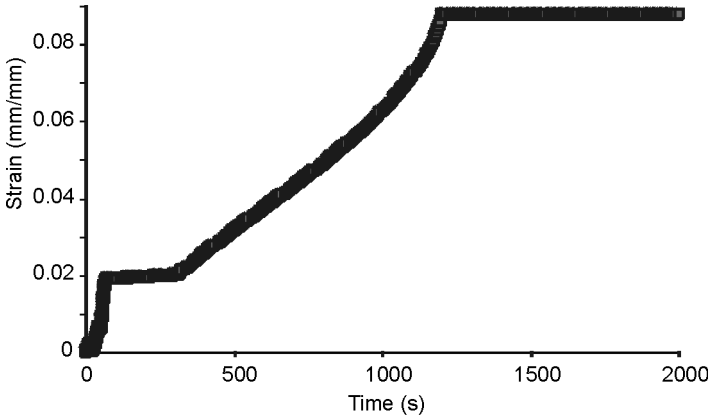

Fig. 11. Creep strain vs. time at 850 °C in creep test

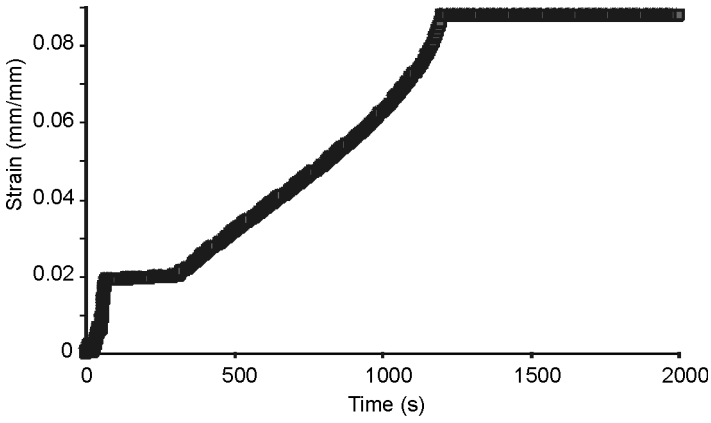

Fig. 12. Creep strain vs. time at 853 °C in creep test

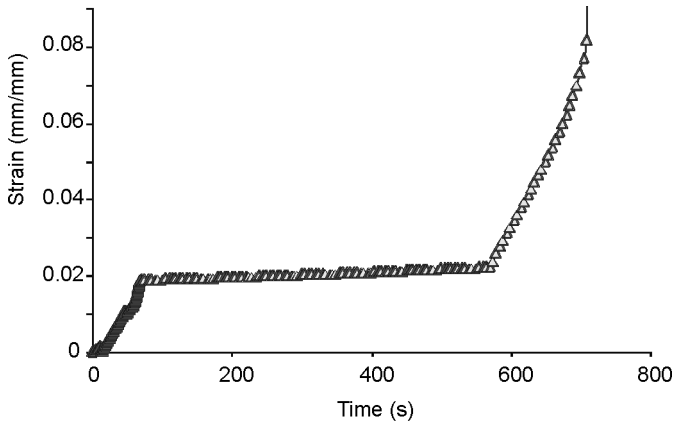

Fig. 13. Creep strain vs. time at 875 °C in creep test

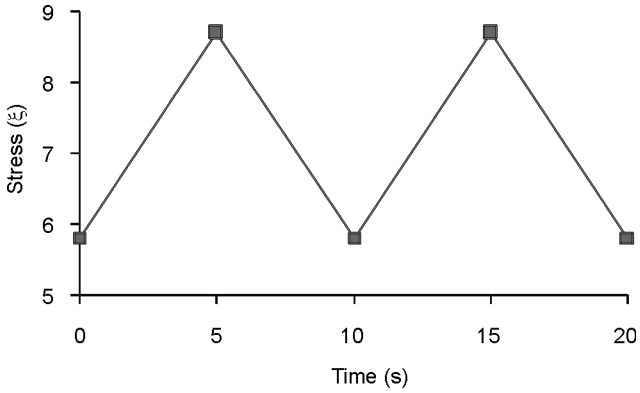

Fig. 14. Stress waveform for fatigue test

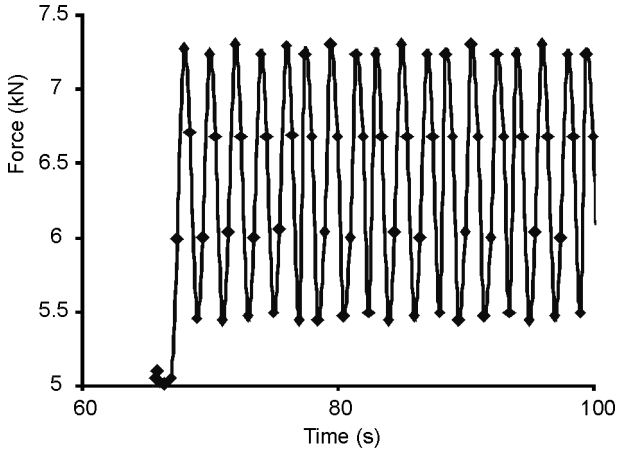

Fig. 15. Force waveform for fatigue test

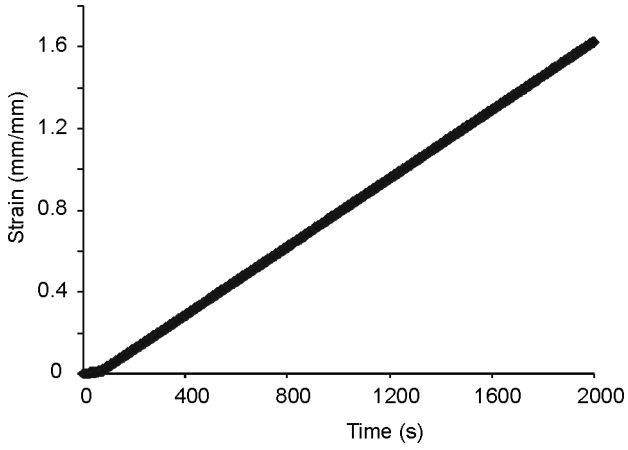

Fig. 16. Strain vs. time in fatigue test

For fatigue, a cyclic load (Fig. 14) was applied on a sample of steel 4340 of 12.7 mm in diameter, 90 mm long until break down. The minimum stress was 40.04 MPa and the maximum stress was 60.10 MPa. Practically we could apply force between 5.07 kN to 7.61 kN (Fig. 15). The total spend time was 2019.5 s and each cycle was 10 s but it took 66 s of preliminary time to start the cyclic load. Then taking the net time for the cyclic load, the number of reversals is obtained. Figure 16 shows the strain vs. time in the fatigue test.

Table 4. Creep test results for steel 4340

Test No.	T [°C]	t_R [s]
1	800	3645
2	850	1205
3	853	1125
4	875	715

Table 5. Creep, fatigue and total damages from model 1 and the test

Model	Creep damage D_c	Fatigue damage D_F	Total damage D_T
Model 1 (test data)	0.01372	0.02476	0.0384786
Model 1 (calculation data)	0.0135448	0.02619596	0.0275504
Test			0.03986

The test data has been used to find the total damage at creep-fatigue interaction. As an example, the damages at 50 s obtained from tests and from the models are shown in Table 5. For the test, cyclic load was applied on a sample of 12.7 mm in diameter 90 mm long steel 4340 until break down. The minimum stress was 40.04 MPa (5.81ξ) and the maximum stress was 60.10 MPa and the hold time was 5 s. The force and temperature were applied and the stress and strain were measured. Practically break down happened after 1254.5 s.

5.1.2. Model 2

Based on the Miners rule for fatigue failure, for the case that was tested we have: σ_a = 10.03 MPa, σ_m= 50.07 MPa, σ_{cr} for 800 °C and 1 h lifetime is 50.7 MPa, S_{ut}= 825 MPa, then $0.9S_{ut}$ = 742.5 MPa. Substituting these values in the Miners equation, we have

$$N_f = \frac{\text{Total spent time}}{\text{period of 1 cycle}} = \frac{1254.5}{15} = 83.6 \tag{28}$$

5.2.3. Model 3

From Equation (25) we have:

$$N_R = N_{SF} = \left[\frac{1}{\frac{1}{N_f} + \frac{t_h}{t_R}} \right] \tag{29}$$

For the case that was tested we have: $N_f = 195.35$, $N_{SF} = 0.54$, $t_h = 5$ s, $t_R = 3645$ s. Using Equation (25) ,the number of cycles to break for the steel 4340 was obtained as

$$N_R = 83.1951 \text{ cycles} \tag{30}$$

The present life status for instance after 50 s which is equivalent to 3.33 cycles, is

$$L_R = 1 - \frac{N}{N_R} = 1 - \frac{3.33}{83.1951} = 0.9599$$

Test result gives

$$N_R = \frac{1254.5}{15} = 83.6 \text{ cycles} \tag{31}$$

The present life status for instance after 50 s which is equivalent to 3.33 cycles, is

$$L_R = 1 - \frac{N}{N_R} = 1 - \frac{3.33}{83.6} = 0.9601 \tag{32}$$

6. Discussion and conclusions

Three constitutive models have been suggested. In the first model, the main idea is that the total damage can be used for break point of the components, and the damages due to creep and fatigue can be accumulated linearly. In this model, the creep model uses the Norton power law, Larson–Miller and Robinson rule approach, while the fatigue model combines the Miner rule and the universal slope method. The damages are calculated separately and the total damage is found by linear summation in order to find the lifetime.

In model 2, the fluctuating stress is considered as a varying stress in the fatigue -creep model. Since the fluctuating stress is a combination of alternating and mean

stress, it can be assumed that the mean part represents the static load which can cause creep at elevated temperatures, whereas the alternating part is responsible for fatigue damage. This model is an extension to the Goodman theory, except that instead of an intercept of ultimate stress (σ_U) on the σ_m axis, the intercept used is the creep-limited static stress (σ_{cr}).

In model 3, the approach for this model is that the creep-fatigue interaction can be considered as cyclic fatigue but with the hold time at maximum, minimum, or extreme stresses. This model has two strong points: 1) the required data can be used from pure creep and pure fatigue tests; 2) it has a safety factor (or a weakness factor) that is based on the material information and industrial experiences, between 0 and 1.

Out of three constitutive models, the first one is the most accurate and reasonable one, although the third one is the easiest one. The main weak point of the second one is that it gives just a range of the lifetime or lifecycle for the low frequency loads, and it cannot be accurate in that region. The weak point of the 3rd one is finding the safety factor accurately. It should be noted that more tests are needed to find the constants in universal slope equation. In the present study, the constants are taken from ASM handbook. For unknown materials, many more tests are needed to find those constants. In the present case, the result of the lifetime prediction in creep-fatigue interaction tests and the first constitutive model has quite reasonable and acceptable match. Three suitable models for predicting the lifetime were developed and studied. The finite element technique was used to study the component dynamic behaviour. Natural frequencies and mode shapes were obtained. The response and stress due to harmonic and centrifugal loading were also obtained. The analytical results were compared with those obtained from experiments.

References

[1] OHTANI R., KITAMURA T., TSUTSUMI M., MIKI H., Proc. Asian Pacific Conf. Fracture and Strength, Tsuchiura (Japan), 1993, pp. 151–156.
[2] EWALD J., SHENG S., Mater. High Temp., 15 (2003), 323.
[3] GRANACHER J., MAO T.S., FISCHER R., Mater. High Temp., 15 (2003), 331.
[4] MAILE K., KLENK A., GRANACHER J., SCHELLENBERG G., TRAMER M., Key Eng. Mater., 171–174 (2000), 85.
[5] KOTEKAZAWA R., Fatigue Fract. Eng. Mater. Struct., 16 (1993), 619.
[6] MICHEL D.J., THOMPSON A.W., Fatigue, 87 (1987), 1057.
[7] WANG S., CHI S., GENG G., Acta Metal. Sin., 20 (1984), 83.
[8] SADANANDA K., SHAHINIAN P., *Creep-Fatigue Crack Growth*, Appl. Sci. Publ., London, 1981, pp. 109–195.
[9] SHAHINIAN P., SADANANDA K., ASME, New York, 1976, pp. 365–390.
[10] GENG M. F., Mater. Sci. Eng., 257 (1998), 250.
[11] MARIE S., DELAVAL C., Intl. J. Press. Vess. Piping, 78 (2001), 847.
[12] GEMMA A.E., Eng. Fract. Mech., 11 (1979), 763.
[13] BRINKMAN C.R., KORTH G.E., BOBBINS R.R., Nucl. Techn., 16 (1972), 297.
[14] YAGI K., KUBO K., TANAKA C., J. Japan Soc. Mater. Sci., 28 (1979), 400.

[15] REIS E.E, RYDER R.H., *Creep-Fatigue Damage in OFHC Coolant Tubes for Plasma Facing Components*, Proc. 19th Symposium on Fusion Technology, 1996.
[16] BELLOWS R.S., TIEN J.K., Scripta Metall., 21 (1987), 653.
[17] RICHARD-FRANDSEN R., TIEN J.K., Scripta Metall., 18 (1984), 731.
[18] DUGGAN T.V., SABIN P., *The Effect of Geometry on Crack Formation, Advances in Research on the Strength and Fracture of Materials*, Proc. 4th International Conference on Fracture, New York, 1978, p. 285.
[19] BERMAN I., GANGADHARAN A.C., JAISINGH G.H., GUPTA G.D., J. Press. Vess. Techn., 98 (1976), 75.
[20] PARK Y.S., NAM S.W., AND HWANG S.K., Mater. Lett., 53 (2002), 392.
[21] HARDT, MAIER H.J, CHRIST H.J., Int. J. Fatigue, 21 (1999), 779.
[22] SALAM I., TAUQIR A., KHAN A.Q., Engineering Failure Analysis, 9 (2002), 335.
[23] BESTWICK R.D.W., BUCKTHORPE D.E., Fatigue Fract. Eng. Mater. Struct., 17 (1994), 849.
[24] HOLDSWORTH S.R., Nucl. Eng. Des., 188 (1999), 289.
[25] ZHANG G., RICHTER B., Fatigue Fract. Eng. Mater. Struct., 23 (2002), 499.
[26] LEMAITRE J., PLUMTREE A., Trans. ASME, 101 (1979), 284.
[27] SHI X.Q., WANG Z.P., ZHOU W., PANG H.L., YANG Q.J., J. Electr. Pack., 124 (2002), 850.
[28] RUBESA D., *Lifetime Prediction and Constitutive Modeling for Creep-Fatigue Interaction*, Bruder-Borntraeger, Berlin, 1996, p. 140.
[29] COLOMBO F., MASSEREY B., MAZZA E., HOLDSWORTH S., *Service-Like Thermo-Mechanical Fatigue Tester for the Lifetime Assessment of Turbine Components*, 9th Int. Conf. Mechanical Behavior of Materials, Geneva, Switzerland, 2003.
[30] HOLDSWORTH S.R., MAZZA E., AND JUNG A., *Creep-Fatigue Damage Development during Service-Cycle Thermo-Mechanical Fatigue Tests of ICrMoV Rotor Steel*, 9th Int. Conf. Mechanical Behavior of Materials, Geneva, Switzerland, 2003.
[31] CHARKALUK E., CONSTANTINESCU A., Mater. High Temp., 17 (2000), 373.
[32] YAO Q., QU J., WU S.X., J. Electr. Pack., 121 (1999), 196.
[33] JEONG C.Y., CHOI B.G., NAM S.W., Mater. Lett., 49 (2001), 20.
[34] CHEN L.J., YAO G., TIAN J.F., WANG Z.G., ZHAO H.Y., Int. J. Fatigue, 20 (1998), 543.
[35] TONG J., DALBY S., BYRNE J., HENDERSON M.B., HARDY M.C., Int. J. Fatigue, 23 (2001), 897.
[36] COFFINE L.F., Fatigue Elev. Temp., ASTM.520, 1973, 5–34.
[37] AGHION E., BAMBERGER M., BERKOVITS A., Israel J. Techn., 24 (1988), 225.
[38] OKADA M., TSUTSUMI M., KITAMURA T., OHTANI R., Fatigue Fract. Eng. Mater. Struct., 21 (1988), 751.
[39] VENKITESWARAN P. K., FERGUSON D. C., AND TAPLIN D.M.R., *Fatigue at Elevated Temperatures*, Proceedings of the Symposium, Philadelphia, PA, ASTM, 462–472, 1973.
[40] OHNAMI M., SAKANE M., Bull. Japan Soc. Mech. Eng., 21 (1978), 547.
[41] KOBURGER C.W, DUQUETTE D.J, STOLOFF N.S., Metall. Trans. A, Phys. Metall. Mater. Sci., 11 A (1980), 1107.
[42] PLUMTREE A., PERSSON N.G., *Creep-Fatigue Interaction in an Austenitic Fe-Ni-Cr Alloy at 600 °C*, Advances in Research on the Strength and Fracture of Materials, Proc. 4th Int. Conf. Fracture, Pergamon Press, New York, 1978, pp. 821–829.
[43] OHTANI R., KITAMURA T., ZHOU W., Int. J. Fatigue, 19 (1997), 185.
[44] SRINIVASAN V.S., NAGESHA A., VALSAN M., BHANU SANKARA RAO K., MANNAN S.L. SASTRY D.H., Int. J. Press. Vess. Piping, 76 (1999), 863.
[45] KORDISCH T., NOWACK H., Fatigue Fract. Eng. Mater. Struct., 21 (1998), 47.
[46] MASAKAZU O., HIROMICHI T., JUNNOSUKE M., Mater. Sci. Res. Int., 3 (1997), 56.
[47] MICHEL D.J., SMITH H.H., Acta Metall., 28 (1980), 999.
[48] WAREING J., TOMKINS B., *Creep-Fatigue Interaction Failure in Type 316 Stainless Steel, Advances in Research on the Strength and Fracture of Mater.*, Proc. 4th Int. Conf. Fracture, New York, Pergamon Press, 1978, 81.

[49] MAIYA P.S., MAJUMDAR S., Metallurgical Transactions A -Physical Metallurgy and Mater. Sci., 8A (1977), 1651.
[50] WAREING J., Metall. Trans. A, 8A (1977), 711.
[51] PLUMTREE A., Metal Sci., 11 (1977), 425.
[52] MILLER A., ASMS, Conf. Micromechanical Modeling of Flowand Fracture, ASME, Transactions, Series H- J. Eng. Mater. Techn., 98 (1976), 106.
[53] NAM S.W., Mater. Sci. Eng., 322 (2002), 64.
[54] ISOBE N., SAKURAI S., YORIKAW.A. M., IMOU K., TAKAHASHI Y., Int. J. Press. Vess. Piping, 77 (2000), 817.
[55] TAKAHASHI Y., OGATA T., TAKE K., Nucl. Eng. Des., 153 (1995), 235.
[56] HALES R., Fatigue Eng. Mater. Struct., 3 (1980), 339.
[57] WAREING J., Fatigue Eng. Mater. Struct., 4 (1981), 131.
[58] JASKE C., MINDLIN H., PERRIN J., ASTM, 520 (1973), 365.
[59] OKAZAKI M., YAMAZAKI Y., Int. J. Fatigue, 21 (1999), 79.
[60] ASME, Boiler and Pressure Vessel Code, Section III, Code Case N-47, 1974.
[61] ROBINSON E.L., ASME Trans., 160 (1938), 253.
[62] MINER M.A., J. Appl. Mech., 12 (1945), A159.
[63] TAIRA S., *Creep in Structures*, Academic Press, 1962, pp. 96–124.
[64] LARSON F.R., MILLER J., ASME Trans., 1952, 765–775.
[65] *Dynamic Systems*, Inc. P.O. Box 1234, Poestenkill, NY, 12140.

Received 13 February 2007
Revised 28 June 2008